Electrochemical capacitance-voltage depth profiling of nanometer-scale layers fabricated by Ga^+ focused ion beam implantation into silicon

H. C. Mogul and A. J. Steckl
University of Cincinnati/Nanoelectronics Laboratory, Cincinnati, Ohio 45221-0030

Gyles Webster
Bio-Rad Microscience Division, Mountain View, California 94043

M. Pawlik
SAS, Ltd., High Wycombe, England H14 3BE

S. Novak
Evans East, Plainsboro, New Jersey 08536

(Received 13 March 1992; accepted for publication 19 May 1992)

The electrochemical capacitance-voltage (ECV) profiling technique is employed to measure the active carrier concentration in nanoscale layers fabricated by focused ion beam (FIB) implantation of 3 to 10 keV Ga^+ ions into crystalline Si. The carrier concentration profiles obtained by ECV indicate the ability of this technique to probe depths as shallow as 2–3 nm and with a nanometer-scale depth resolution. The carrier concentration obtained by ECV matches well with the Ga atomic concentration profile detected by secondary-ion mass spectroscopy, but is almost an order of magnitude higher than that provided by the spreading resistance profile technique.

Characterization of electrically active carrier profiles of heavily doped and shallow ($\leqslant$100 nm) layers of Si presents a challenging analytical task[1] towards the development of various semiconductor devices and, in particular, sub-micro meter CMOS technology. Ga^+ focused ion beam (FIB) implantation has resulted in the fabrication of shallow *p*-type layers and *p-n* junctions. This is due to the low amorphization dose produced by the large atomic mass of ^{69}Ga, which (a) allows solid-phase regrowth with a low thermal processing budget, hence minimizing diffusion; (b) results in a low percentage of channeling even at very low implant energies.[2,3] The use of FIB implantation[4] provides the flexibility of a localized doping process, without the need for a mask or lithography.

Recently, the profiling of low energy Ga implants by secondary-ion mass spectroscopy (SIMS) has been reported[5] to provide a depth resolution as high as 1–2 nm. However, this chemical dopant profile does not always give a good indication of the electrically active carrier concentration, which is critical for accurate device performance prediction. In order to measure the active carrier concentration, techniques such as spreading resistance profiling[6] (SRP) or electrochemical capacitance-voltage[7–9] (ECV) profiling have been employed. ECV provides an elegant method for the determination of near-surface active dopant concentration, while the electrochemical etching of the original sample surface provides the depth profiling capability. The method employs the relationship between the applied reverse-bias voltage, the width of the resulting space charge region, and the carrier concentration. The latter is inversely proportional to the derivative of the *C-V* curve (i.e., dC/dV). The equations governing this method are available from standard semiconductor texts.[10]

Ga^+ FIB implantation was performed perpendicularly on *p*-Si wafers with ⟨100⟩ orientation and background doping of $(3–6)\times10^{15}$ cm^{-3}. The operation of the FIB system is described elsewhere.[2] Implantations were performed at 3, 5, and 10 keV within an area of size 500×500 μm^2 with doses ranging from 10^{13}–10^{15} cm^{-2}, using an unseparated Ga beam of 400 pA. After the implant, solid-state regrowth was achieved by RTA at 600 °C for 30 s in N_2. Companion samples were prepared under the same conditions for SIMS and SRP analysis.

ECV analysis was carried out with a BioRad profiler PN4300.[11] This technique uses a defined area of electrolyte contact to the semiconductor surface to form a zero-bias (or slightly forward bias) depletion region. An ac signal is superimposed onto the dc bias to measure the capacitance and hence the carrier concentration of the semiconductor material. This modulation signal enables the depletion width to be calculated without ramping the dc bias. Depth profiling is achieved by the electrochemical etching of the semiconductor material under the electrolyte "Schottky" contact. For samples used in this experiment, the sealing ring used to define the electrolyte contact area was larger than 500×500 μm^2 windows in the oxide, hence a contact area of 0.0025 cm^2 was used in the calculations for carrier concentration and etch depth. The electrolyte used was a 0.1 M solution of $NH_4F\cdot HF$.

Figure 1 shows representative ECV profiles for samples implanted with 10 keV Ga^+ ions at doses of 10^{14} and 10^{15} cm^{-2}. As can be seen, the carrier concentration can be obtained as close as 2–3 nm below the original surface and with a nanometer-scale depth resolution. In the near-surface regions, both implant doses result in active carrier concentrations above the solid solubility[12] of Ga ions annealed at 600 °C ($\approx7–8\times10^{18}$ cm^{-3}). The difference in the minimum ("bulk") concentration in the two profiles in Fig. 1 arises from two ECV modes of operations. In the normal mode, the Schottky diode is held at zero or a slightly small forward bias, as explained above. A disadvantage of this mode is that the electrochemical etching

 0003-6951/92/300554-03$03.00

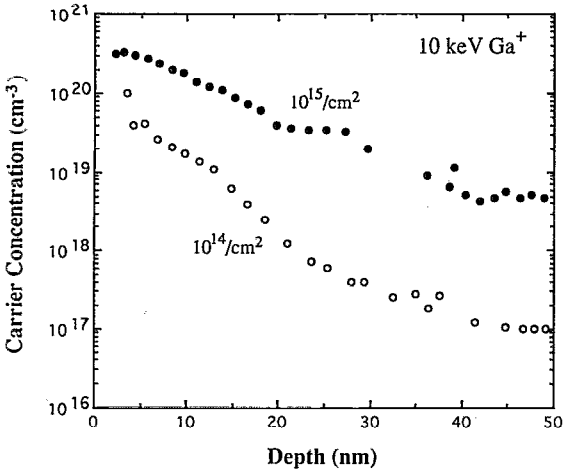

FIG. 1. ECV carrier-concentration profile for 10 keV Ga^+ FIB implantation into Si at doses of 10^{14} and 10^{15} cm^{-2} and annealed at 600 °C for 30 s.

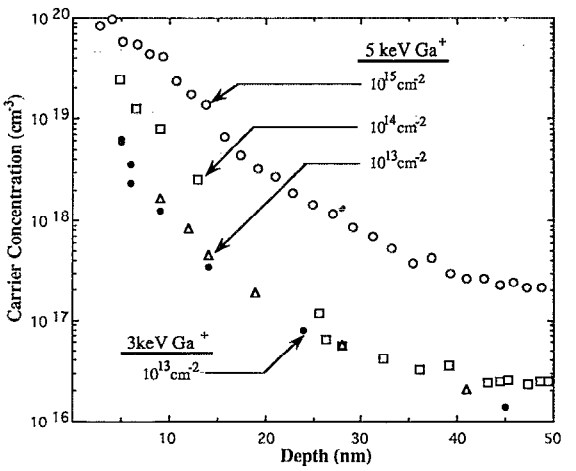

FIG. 2. ECV carrier-concentration profile for 5 keV Ga^+ FIB implantation into Si at doses of 10^{13}, 10^{14}, and 10^{15} cm^{-2} and 3 keV Ga^+ at a dose of 10^{13} cm^{-2}. RTA at 600 °C for 30 s.

can take from several minutes to one hour, depending upon the thickness of the material being removed. In the second, less common, mode the bias voltage is rapidly stepped in the reverse-bias direction to increase the depletion width and hence profile the carrier concentration with minimum etching of the surface. This is a much faster measurement, but it works only for low-to-moderate concentrations due to breakdown. In these experiments, the samples with lower doses (i.e., 10^{13} and 10^{14} cm^{-2}) were of sufficiently low concentrations such that the fast depletion profile mode was used. Under these conditions, the electrolyte was in contact with the oxide for a short time and the background capacitance arising from the electrolyte/oxide/semiconductor structure was small. For the sample implanted with a dose of 10^{15} cm^{-2}, the fast depletion profile was not possible, and hence, the longer ECV profiling was necessary. In this case, the electrolyte resulted in a considerable amount of oxide thinning. In turn, this resulted in a higher background capacitance, and hence, a higher background concentration.

Figure 2 compares the ECV carrier concentration profiles for the 5 keV implanted samples at doses of 10^{13}, 10^{14}, and 10^{15} cm^{-2} and a 3 keV sample implanted with a dose of 10^{13} cm^{-2}. The ECV technique clearly distinguishes the effect of dose on concentration profile in the near-surface ($\leqslant$15 nm) region. However, no effect is observed due to a reduction in energy from 5 to 3 keV at the low dose of 10^{13} cm^{-2}. Figure 3 shows the depth of a 10 keV Ga implant with a dose of 1×10^{14} cm^{-2} as determined from ECV, SIMS, and SRP. The good agreement between the atomic concentration profile provided by SIMS and the carrier concentration profile as measured by the ECV technique indicates that the majority of the implanted ions are electrically active. This agreement does not extend to the first 1–2 nm below the surface because of transient effects in the SIMS analysis. The SRP-obtained concentration indicates a significant difference with the ECV and SIMS data at depths less than ~20 nm. In general, there are a number of factors that limit SRP profiling of ultrashallow ($\leqslant$25 nm) regions. Some of the more serious limitations include carrier spilling, shallow angle bevels which affect the carrier distribution, and crystalline imperfections which can lead to noise problems due to a small sampling volume. SRP measurements also involve detailed interpretation due to the need for correction factors. Furthermore, SRP measurements require an accurate knowledge of the effective carrier mobility as a function of concentration. In the SRP profile shown in Fig. 3, an effective value for the hole mobility of standard (boron-doped) p-type Si is assumed since the hole mobility in shallow layers obtained by low-energy Ga implantation is not known. However, the hole mobility of Ga^+-doped Si has been shown[13,14] to be at least a factor of 2–10 times less than that for B-doped Si in regions with concentrations of 10^{19}–10^{21} cm^{-3}. In contrast, ECV measurements do not involve such difficulties and the data is unambiguous, providing the carrier concentration of the implanted regions without dependence on mobility. However, since the implantation is performed in p-Si, junction depths cannot be obtained by ECV measurements.

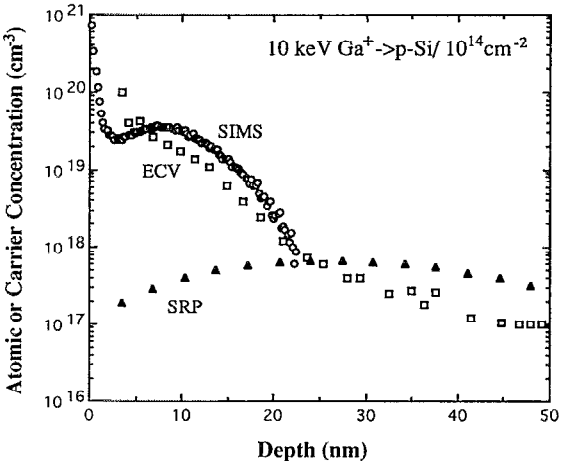

FIG. 3. The comparison of depth distribution for 10 keV Ga^+ FIB implantation into Si at a dose of 1×10^{14} cm^{-2} as determined by ECV, SIMS, and SRP techniques under similar processing conditions.

In conclusion, the effectiveness of the ECV technique for profiling shallow layers of nanometer dimensions has been demonstrated. ECV results have been compared with SIMS and SRP data. The ECV technique is shown to be relatively straightforward, as it does not involve some of the complexities required by the other techniques. Nevertheless, no one technique can be deemed exclusive, as each provides useful information towards the ultimate goal of analyzing nanometer-scale layers.

[1] W. Vandervost and T. Clarysse, J. Vac. Sci. Technol. B **10**, 302 (1992).
[2] A. J. Steckl, H. C. Mogul, and S. Mogren, J. Vac. Sci. Technol. B **8**, 1937 (1990).
[3] A. J. Steckl, H. C. Mogul, S. W. Novak, and C. W. Magee, J. Vac. Sci. Technol. B **9**, 2916 (1991).
[4] J. Melngailis, J. Vac. Sci. Technol. B **5**, 469 (1987).
[5] S. W. Novak, C. W. Magee, H. C. Mogul, A. J. Steckl, and M. Pawlik, J. Vac. Sci. Technol. B **10**, 333 (1992).
[6] M. Pawlik, J. Vac. Sci. Technol. B **10**, 388 (1992), and references therein.
[7] N. Sieber, H. E. Wulf, D. Roser, and P. Kurps, Phys. Status Solidi A, **126**, K123 (1991).
[8] P. Blood, Semicond. Sci. Technol. **1**, 7 (1986).
[9] C. D. Sharpe, P. Lilley, C. R. Elliot, and T. Ambridge, Electron. Lett. **15**, 622 (1979).
[10] D. K. Schroder, *Semiconductor Material and Device Characterization* (Wiley, New York, 1990).
[11] I. C. Mayes, Bio-Rad Semiconductor Note No. 202 (1985).
[12] *Quick Reference Manual for Silicon Integrated Circuit Technology*, edited by W. E. Beadle, J. C. Tsai, and R. D. Plummer (Wiley, New York, 1985).
[13] M. Y. Tsai, B. G. Streetman, V. R. Deline, and C. A. Evans, J. Electron. Mater. **8**, 111 (1979).
[14] Y. Sasaki, K. Itoh, E. Inoue, and T. Mitsuishi, Solid-State Electron. **31**, 5 (1988).